Heavy-ion fusion-evaporation reactions: high spin states in ^{43}Ca and ^{43}Sc†

A. R. Poletti*
University of Auckland, Auckland, New Zealand

E. K. Warburton, J. W. Olness, J. J. Kolata, and Ph. Gorodetzky‡
Brookhaven National Laboratory, Upton, New York 11973
(Received 2 September 1975)

Fusion-evaporation reactions, primarily ^{27}Al(^{19}F,$n2p$)^{43}Ca and ^{27}Al(^{19}F,$2np$)^{43}Sc, have been used to investigate the structure and formation of the residual nuclei. Decay schemes of the yrast levels which are populated are presented together with suggested spin assignments for some of the higher levels. Incidental results obtained for the nuclei ^{44}Ca, ^{44}Sc, and ^{40}Ca are also discussed. Mean lifetimes measured by the recoil distance method are as follows: (^{43}Ca): 2754-keV level, $\tau = 34.1 \pm 1.5$ psec; 990-keV level, $\tau = 73 \pm 11$ psec; (^{43}Sc): 880-keV level, $\tau = 7.0 \pm 1.4$ psec; 472-keV level, $\tau = 233 \pm 53$ psec; (^{44}Ca): 3285-keV level, $\tau = 23 \pm 7$ psec, 2283-keV level, $\tau < 25$ psec; (^{44}Sc): 631-keV level, $\tau = 550 \pm 80$ psec; 3567-keV level, $\tau = 51 \pm 10$ psec. The properties of the high spin states populated in the ^{19}F + ^{27}Al fusion-evaporation reaction are discussed. Relative excitation intensities of the residual nuclei are interpreted in terms of a Hauser-Feshbach calculation, while a simplified pairing force model allows us to explain a number of observations in specific nuclei.

[NUCLEAR REACTIONS ^{27}Al(^{19}F, $2pn$)^{43}Ca and ^{27}Al(^{19}F, $p2n$)^{43}Sc. $E = 40$ MeV; measured γ-γ coinc, $\sigma(E_\gamma, \theta)$, $P(E_\gamma, \theta = 90°)$, and $T_{1/2}$ for γ transitions; deduced decay schemes and Λ for transitions and J^π, δ for high-spin levels. Additional data on ^{44}Ca, ^{44}Sc, and ^{40}Ca.]

I. INTRODUCTION

The data we report here were obtained as part of an extensive experimental investigation[1,2] of fusion-evaporation reactions leading to excited final nuclei in the upper part of the $2s$-$1d$ shell and the lower part of the $1f$ shell. The investigations employed Ge(Li) spectroscopy to study the reaction γ rays produced by bombardments involving projectiles ($A \leq 19$) incident on targets ($A \leq 28$) in the projectile energy range $20 \leq E \lesssim 60$ MeV.

From these studies a large amount of information on the structure of nuclei ranging in mass from $37 \leq A \lesssim 44$ was obtained,[1-8] and a broad survey of the data is given in Refs. 1 and 2. As could be expected, certain final nuclei were produced more stongly in some reactions than in others, and detailed analyses for some of these cases have been presented: ^{39}K (Refs. 4 and 2); ^{41}K and ^{41}Ca (Refs. 2 and 3); ^{42}K and ^{42}Ca (Ref. 7); ^{44}Ti and ^{44}Sc (Ref. 5); ^{42}Ca and ^{43}Ca (Ref. 6); and ^{38}Ar (Ref. 8).

The nuclei ^{43}Ca and ^{43}Sc were formed most strongly in the bombardment of ^{27}Al by ^{19}F, via the ^{27}Al(^{19}F, $2pn$)^{43}Ca and ^{27}Al(^{19}F, $p2n$)^{43}Sc reactions, and we now consider the results obtained for these nuclei in detail. Some incidental information is also presented on ^{44}Ca and ^{44}Sc, formed via the two-particle ($2p$) and (pn) exit channels, and on ^{40}Ca formed via the three-particle ($\alpha 2n$) exit channel. These results will subsequently be compared with additional evidence on these final state nuclei available from other experiments, as will be discussed. In addition the relative excitation intensities for the residual nuclei will be discussed in terms of a simplified pairing force model which is used to calculate the positions of the yrast levels in these nuclei.

II. EXPERIMENTAL PROCEDURE

Although the nuclei ^{43}Sc and ^{43}Ca were formed most strongly in the ^{19}F on ^{27}Al bombardment, additional supportive evidence is available from other reactions[1,2] and, in fact, has been used in arriving at our final conclusions on the level structure of these nuclei.

Five different experimental techniques were used in the investigation of the ^{19}F + ^{27}Al reaction γ rays:

(i) Yield curves for various discrete γ-ray lines were measured for $\theta_\gamma = 90°$ over the range of ^{19}F bombarding energies $20 \leq E_B \leq 45$ MeV. A target consisting of 350 μg/cm^2 of aluminum evaporated on a tungsten backing was used, and the bombarding energy was varied in steps of 5 MeV.

(ii) Angular distributions were measured at a bombarding energy of 40 MeV using the same

target. Data were obtained with a Ge(Li) detector at detection angles θ_γ, measured relative to the beam direction, of 0°, 25°, 35°, 45°, 55°, 65°, and 90° and were normalized according to the yield in a second monitor detector placed at $\theta_\gamma = 90°$. A beam current of ~70 nA of $^{19}F^{5+}$ ions was used and the runs at each angle lasted approximately one hour.

(iii) A two-crystal Ge(Li) Compton polarimeter placed at $\theta_\gamma = 90°$ was used to measure the linear polarization of the reaction γ rays. The polarimeter axis was rotated automatically at ~5-min intervals, so as to spend equivalent amounts of time in the two orientations (perpendicular and parallel) relative to the reaction plane. The target and bombarding energy were the same as for (ii) so that the nuclear alignments of the γ-emitting states are also the same.

(iv) The recoil distance method (RDM) was employed to measure the lifetime of a number of excited states with lifetimes in the range from 7 to 550 psec. A 36-MeV beam of $^{19}F^{4+}$ ions, at a beam current of ~150 nA, was used to bombard a stretched aluminum foil 250 $\mu g/cm^2$ thick. Measurements were made for a total of 12 target-stopper distances between 0 and 5.7 mm, with each Ge(Li) spectrum requiring about 40 min of bombardment.

(v) A γ-γ coincidence experiment using two Ge(Li) detectors was performed using a thick Al target at a ^{19}F bombarding energy of 45 MeV. The measurement required ~24 h at a $^{19}F^{5+}$ beam current of 15 nA. Individual events corresponding to an 8192× 8192 channel matrix were recorded on magnetic tape and were subsequently analyzed by sorting into the various spectra seen by one detector in coincidence with sharp lines observed in the other.

With respect to (ii) and (iii) we note that detailed experimental results for $^{19}F + ^{27}Al$ have been tabulated,[1,2] and further that examples of the general procedures of analysis have also been illustrated in considerable detail.[1-8] It is not our point to recapitulate the details of the method—rather, we wish merely to indicate the general philosophy of the analysis procedure.

The identification of the various lines of the γ spectrum is based primarily on the results of (i) and (v). The yield curve indicates which of the stronger γ rays are most likely to arise from one-, two-, or three-particle emission in the exit channels, since these processes peak at measurably different bombarding energies. The $\gamma\gamma$ coincidence measurement then establishes that specific (frequently weaker) lines are in coincidence with stronger transitions connecting known low-lying levels in a given final nucleus. These identifications have been indicated previously,[1,2] and in conjunction with the relative intensities determined for the various lines via (i), the decay scheme and branching ratios for each nucleus as populated in the $^{19}F + ^{27}Al$ fusion-evaporation reaction could be deduced. Figures 1 and 2 give the decay schemes for ^{43}Ca and ^{43}Sc resulting from this work.

Further analysis of these data was facilitated by the fact that many of the nuclear states of interest are relatively long-lived, i.e., >1 psec. In the absence of measurable Doppler broadening, the various spectral lines exhibit the characteristic detector line shape, and thus semiautomatic peak-fitting routines were used to extract intensities as a function of the experimental parameter being varied in (i)—(v).

The angular distribution data, after suitable normalization, were fitted with the even order Legendre polynomial expansion

$$W(\theta) = A_0[1 + a_2P_2(\theta) + a_4P_4(\theta)].$$

The relative intensity was then obtained in terms of the peak areas A_0 as $I = A_0/\epsilon(E_\gamma)$, where $\epsilon(E_\gamma)$ is the relative photo-peak efficiency of the Ge(Li) detector.

For the nuclei ^{43}Ca, and ^{43}Sc the appropriate entries have been abstracted from Ref. 1 and are presented and identified in Tables I and II,

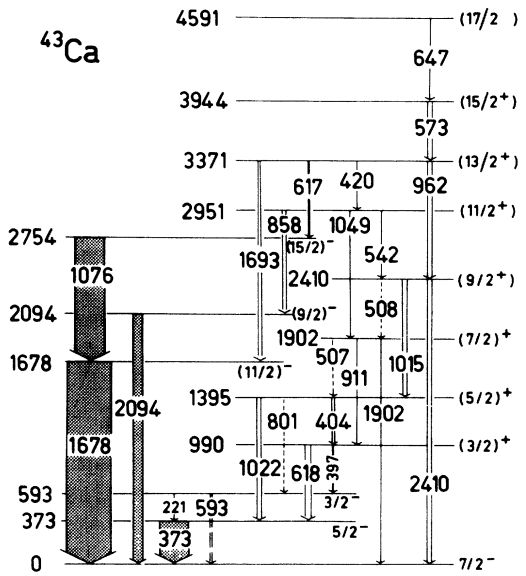

FIG. 1. The level scheme of ^{43}Ca as deduced from its excitation by the $^{27}Al(^{19}F, n2p)^{43}Ca$ reaction at 40 MeV. The widths of the arrows signifying observed transitions are proportional to their relative intensities. Transitions reported by other workers and indicated by dashed lines were too weak to be observed in the present experiments.

respectively. These tables also summarize the linear-polarization data taken from Ref. 2.

For the RDM data the intensities I_0 and I_s of the appropriate stopped and shifted γ-ray peaks were determined as a function of the target-stopper distance, and the ratio $R = I_0/(I_0+I_s)$ was formed. In the simplest case R depends on the mean life of the initial level in the following manner:

$$R = \exp[-(D - D_0)/\bar{v}\tau],$$

where $\bar{v}$ is the average recoil velocity, D_0 is the reading on the micrometer corresponding to zero target-to-stopper distance, and D is the corresponding reading when the stopper is displaced a distance $(D - D_0)$ from the target. There is often a distance independent background resulting in an R that is not zero at $D - D_0 = \infty$. We therefore used an iterative nonlinear least squares code to fit $R = A\exp(-D/\bar{v}\tau) + B$ to the data, leaving the quantities A, B, and τ to be determined by the fitting procedure. For some of the transitions we could obtain only I_0. However, given a suitable normalization N, the quantity $R = I_0/N$ contains the same lifetime information as R and could be analyzed subsequently in the same manner. The average recoil velocity $\bar{v}$ was obtained from the difference in energy between the shifted and stopped peaks. We used an average of a number of such determinations and took $\bar{v} = (0.0234 \pm 0.0003)c$, where c is the velocity of light. This agreed quite well with the center of mass recoil velocity calculated from the reaction kinematics ($\bar{v} = 0.0240c$) and was used in the analysis of all lifetimes measured using the $^{19}F + ^{27}Al$ reaction.

III. EXPERIMENTAL RESULTS

In this section we will present the results we have obtained for the nuclei ^{43}Ca and ^{43}Sc, interpret them, and synthesize them with information obtained by other workers. In addition we present some incidental results obtained for levels in ^{40}Ca, ^{44}Ca, and ^{44}Sc. To avoid confusion we emphasize that the results presented in this section are independent of any model predictions of energy level spectra or electromagnetic transition rates.

A. Results for ^{43}Ca

Analysis of the coincidence and angular distribution data enabled us to construct the decay scheme shown in Fig. 1. The widths of the arrows signifying the γ-ray transitions are proportional to the intensity observed in the present work at a bombarding energy of 40 MeV. For the levels below an excitation energy of 1600 keV we adopt the spin assignments compiled by Endt and Van der Leun.[9] The two levels above 3.5 MeV excitation were previously unobserved. Between 1.6 and 3.5 MeV excitation the spin assignments are a synthesis of our present results and those of Alenius *et al.*[10] The assignments for $E_x > 1600$ keV are based on arguments[11] dependent on details of the reaction mechanism, which have not been specifically verified for the individual cases and the assignments are therefore enclosed in parentheses. The argument very briefly is that, in fusion-evaporation or (α, n) reactions, high-spin states in the residual nuclei are populated with a high degree of alignment perpendicular to the beam direction. Because of this the angular distributions and linear polarization measurements can be interpreted in terms of γ-ray emission from levels which are predominantly populated in low magnetic substates. In numerous cases where this can be checked, the hypothesis is verified. Furthermore, we rely heavily on the fact that heavy ion (HI) fusion-evaporation reactions tend to populate yrast levels (i.e., levels of a given spin-parity lying lowest in excitation energy). Essentially, then, we have to distinguish between $J+1 \rightarrow J$ transitions (with $a_2 \simeq -0.3$, $a_4 = 0$ for pure dipole transitions) and $J+2 \rightarrow J$ transitions (with $a_2 \simeq +0.4$, $a_4 \simeq -0.1$ for pure quadrupole transitions). Of course, the possibility of mixed transitions and/or the formation of non-yrast levels must always be kept in

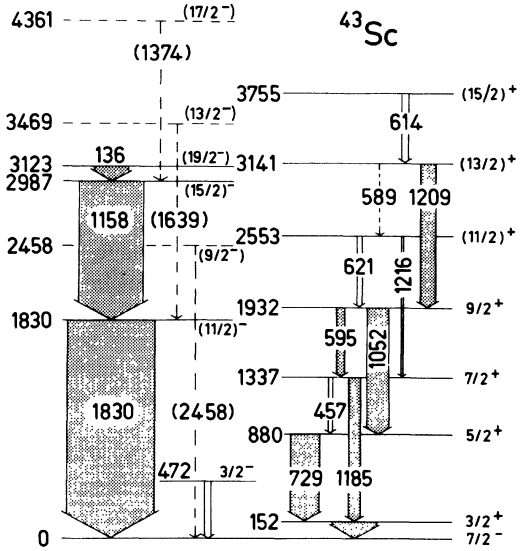

FIG. 2. The level scheme of ^{43}Sc as deduced from its excitation by the $^{27}Al(^{19}F, 2np)^{43}Sc$ reaction at 40 MeV. The widths of the arrows signifying observed transitions are proportional to their relative intensities. Three high-spin states and their γ-ray decays reported by other workers, but too weak to be observed in the present experiment, are indicated by dashed lines.

TABLE I. γ-ray transitions in ^{43}Ca populated in the ^{27}Al(^{19}F, $n2p$)^{43}Ca reaction at 40 MeV.

E_i (keV)	E_f (keV)	E_γ [a] (keV)	J_i^π	τ (psec)	Relative intensity	Multipolarity	Ang. distr. coeffs. a_2 (%)	a_4 (%) [b]	Linear polarization Exp. (%)	Pred. (%)
372.81 (5)	0	372.81 (N)	$\frac{5}{2}^-$	50 ± 4 [c]	~24 000	$M1/E2$ [d]	Radioactive			
593.39 (8)	373	220.58 (N)	$\frac{3}{2}^-$	114 ± 5 [c,e]	1329	$M1/E2$ [f]	−11 (5)	0		
990.32 (7)	593	396.93 (N)	$(\frac{3}{2})^+$	66 ± 3 [g]	1700	···	···	···		
	373	617.51 (N)			6438 [h]	$E1$ [i]	−21 (4)	0	11 (9)	28 (6)
1394.60 (9)	990	404.15 (N)	$(\frac{5}{2})^+$	3.7 ± 1.0 [j]	1983	($M1$)	−25 (5)	0		
	373	1021.78 (N)			4149	···	8 (4)	0		
1677.80(20)	0	1677.76 (N)	$(\frac{11}{2}^-)$	1.2 ± 0.2 [k]	(47 ± 16) × 10^3	($E2$) [l]	23 (2) [m]	−8(2) [m]	30 (8)	34 (6)
1901.80(20)	990	911.49 (N)	$(\frac{7}{2}^+)$	0.80 ± 0.15 [k]	~630 [h]	($E2$)	28 (2)	−16(2)	53(14)	40 (6)
	0	1901.75 (N)			3402	($E1$)	17 (6)	−13(6)		
2093.90(20)	0	2093.85 (N)	$(\frac{9}{2}^-)$	1.8 ± 0.6 [k]	<8453 [n]	($M1/E2$) [o]	−11 (3)	11(3)	−5(22)	
2409.80(20)	1394	1015.19 (N)	$(\frac{9}{2}^+)$	1.8 ± 0.7 [k]	~3630 [h]	($E2$)	35 (2)	−12(2)	19(15)	57 (6)
	0	2409.73 (N)			3713	($E1$)	−23 (5)	0		
2753.96(25)	1678	1076.15(15)	$(\frac{15}{2}^-)$	34.5 ± 1.4 [p]	27 045	($E2$) [q]	25 (2)	−11(2)	43 (7)	36 (6)
2951.49(30)	2409	541.58(30)	$(\frac{11}{2}^+)$	<20 [r]	976	($M1$)	−46(19)	0		
	2094	857.65(25)			3302	···	−9(10)	0		
	1902	1049.06(40)			~1000	···	···	···		
3371.19(42)	2951	419.70(30)	$(\frac{13}{2}^+)$	<20 [r]	2500	($M1$)	−16(12)	0	−41(13)	−22(17)
	2754	617.23 (N)			~1300 [h]	···	···	···		
	2409	961.60(20)			4126 [h]	($E2$)	23 (5)	−10(5)		
	1678	1693.36 (N)			~1000	···	···	···		
3943.84(47)	3371	572.64(20)	$(\frac{15}{2}^+)$	<5 [r]	4034	($M1$)	−25 (5)	0	−8 (5)	−33 (7)
4591.01(56)	3944	647.17(30)	$(\frac{17}{2})$		1351	($M1$ or $E1$)	−17 (7)	0		

[a] An N in place of an uncertainty means the γ-ray energy was calculated from the level separation.

[b] A zero with no uncertainty indicates that the fit was not improved by inclusion of a $P_4(\cos\theta)$ term.

[c] Reference 14.

[d] $|\delta|^2 < 0.07$ (Ref. 13); $\delta = 0.18 \pm 0.05$ (R. N. Horoshko, C. Towsley, and D. Cline, in *The Structure of $1f_{7/2}$ Nuclei*, edited by R. A. Ricci (Editrice Compositori, Bologna, 1971), p. 419.

[e] Reference 15.

[f] $|\delta|^2 < 0.05$ (Ref. 13).

[g] A weighted average of results in Refs. 14, 15, and the present work.

[h] Estimated by comparison with branching ratios given in Ref. 10.

[i] $|\delta| \leq 0.025$ [S. L. Tabor, D. P. Balamuth, and R. W. Zurmuhle, Bull. Am. Phys. Soc. 19, 1034 (1974)].

[j] An average of results in Refs. 15 and k (below).

[k] H. Gruppelaar and P. J. M. Smulders, Nucl. Phys. A179, 737 (1972).

[l] $\delta = 0.05 \pm 0.07$ (Ref. 10).

[m] Transition not resolved from one of similar energy in ^{41}K.

[n] Unresolved from ^{27}Al contaminant.

[o] $\delta = 1.07^{+0.16}_{-0.17}$ (Ref. 10).

[p] An average of results in K. P. Lieb and M. Uhrmacher, Z. Phys. 267, 399 (1974); and present work.

[q] $\delta = 0.05^{+0.05}_{-0.04}$ (Ref. 10).

[r] Limits from present work.

TABLE II. γ-ray transitions in ^{43}Sc populated in the ^{27}Al(^{19}F, $2np$)^{43}Sc reaction at 40 MeV.

E_i (keV)	E_f (keV)	E_γ [a] (keV)	J_i^π	τ	Relative intensity	Multipolarity	Ang. distr. coeffs. a_2 (%)	a_4 (%) [b]	Linear polarization Exp. (%)	Pred. (%)
151.58(15) [c]	0	151.55(15)	$\frac{3}{2}^+$	632 ± 8 msec [d]	...	$M2$	...	...	...	...
472.46(19) [c]	0	472.50(20)	$\frac{3}{2}^-$	230 ± 20 psec	2700	$E2$	9 (3)	−9 (3)	11(19)	8 (7)
880.45(30)	152	728.70(15)	$\frac{5}{2}^+$	6.4 ± 0.9 psec [e]	13 496	$M1/E2$ [f]	−52 (2)	0	23 (6)	2 (4) [f]
1337.16(28)	880	456.82(12)	$\frac{7}{2}^+$	1.2 ± 0.5 psec [d]	2250	$M1/E2$ [g]	−27(10)	0		
	152	1185.07(50)			4714	$E2$ [h]	10 (3)	0	−21(21)	15 (6)
1829.84(30)	0	1829.80(30)	$(\frac{11}{2})^-$	320 ± 40 fsec [d]	42 589	$E2$	16 (1)	−6 (1)	43 (9)	22 (3)
1932.21(50)	1337	595.05(N)	$\frac{9}{2}^+$	3.4 ± 0.8 psec [i]	[3454]	$M1/E2$ [j]	−41 (9)	0	−19(12)	−22(10) [j]
	880	1051.76(40)			9682	$E2$	23 (3)	−5 (3)	16 (9)	36 (8)
2552.89(37)	1932	620.75(30)	$(\frac{11}{2})^+$	740 ± 100 fsec [i]	1748	$M1/E2$ [k]	−51(15)	0	...	...
	1337	1215.66(40)			1188	($E2$)	37(10)	0	...	...
2987.39(34)	1830	1157.55(15)	$(\frac{15}{2})^-$	8.1 ± 1.1 psec [l]	48 336	$E2$	22 (4)	−18 (4)	26 (6)	26(10)
3123.19(39)	2987	135.80(20) [n]	$(\frac{19}{2}^-)$ [n]	650 ± 20 nsec [d]	14 603	$E2$ [n]	...	...	...	...
3141.25(71)	1932	1209.04(50)	$(\frac{13}{2})^+$	...	5744	$E2$	29 (5)	−8 (5)	63(28)	46(12)
3754.95(75)	3141	613.70(25)	$(\frac{15}{2})^+$	...	2704	$M1/E2$ [m]	−73(10)	28(10)	−23(15)	[−23(15)] [m]

[a] An N in place of the uncertainty means the γ-ray energy was calculated from the level separation.
[b] A zero with no uncertainty indicates the fit was not improved by inclusion of a $P_4(\cos\theta)$ term.
[c] Weighted average of values quoted in Refs. 1 and 9.
[d] Reference 9.
[e] Weighted average of results of present work and those reported in Refs. 19 and 20.
[f] $\delta = 0.56 \pm 0.07$, weighted average of results quoted in Ref. 16.
[g] $\delta = 0.28 \pm 0.10$, Ref. 9.
[h] Measured linear polarization disagrees with this, see text.
[i] Ball *et al.*, Refs. 19 and 20.
[j] $\delta = 0.14 \pm 0.06$, Ref. 9.
[k] $\delta = 0.20 \pm 0.07$, Ref. 9.
[l] Reference 22.
[m] $\delta = 0.11 \pm 0.08$ (from present linear-polarization measurements).
[n] From Ref. 17.

mind. A detailed description of some of the methods used to make spin-parity assignments in γ-ray studies of HI fusion-evaporation reactions has recently been published by Taras and Haas.[12]

We summarize in Table I the data we have obtained on the γ-ray transitions in ^{43}Ca together with results by other workers. Column 3 gives the observed γ-ray energy, column 1 gives the level energy derived from it (the recoil correction was applied to the γ-ray energies), and column 2 gives the level to which the transition proceeds. For the first eight listed levels, all energies are derived from the level energies compiled by Endt and Van der Leun[9] not only because of the high accuracy of previous measurements but because in some cases the γ-ray decays from these levels were unresolved from contaminant peaks (see Ref. 1) in the present work. For the higher-lying levels the energies are from the present results. The fourth column gives the spin-parity assignment, while the mean lifetimes are collected in the next column. The observed relative intensity and the angular distribution coefficients are given in columns 6, 8, and 9, while the measured or deduced multipolarity of the transition is given in column 7. The last two columns list, respectively, the linear polarization at 90° as quoted in Ref. 2 and the polarization predicted from the entries of columns 7–9. [This is not the same as the corresponding column in Ref. 2 which gives the prediction for pure (assumed) $M1$ or $E2$ radiation.] Note that the information in columns 3, 6, 8, and 9 is compiled in Ref. 1.

Most of the data in Table I is in agreement with the spin-parity assignments of Fig. 1; we will only comment on a few anomalies. For two of the transitions (2410 → 1395 and 3944 → 3371), the measured linear polarization although having the correct sign is rather smaller than the predicted value. The first of these transitions is, however, contaminated to some extent by a line of similar energy in ^{27}Al, while the second transition could possibly have some $E2$ component. The transition of 396.93 ± 0.11 keV from the 990-keV level is clearly contaminated by the transition of 396.26 ± 0.12 keV from ^{44}Sc. The latter transition is known to be $E2$, which gives rise to the a_4 coefficient reported in Ref. 1: The corresponding entry has therefore been omitted from Table I. A similar problem exists for the ground-state transition from the 1902-keV level. The measured lifetime[13] implies that this $(\frac{7}{2})^+$ to $\frac{7}{2}^-$ transition can have no significant $M2$ component and hence again a_4 should be zero.

From an analysis of the RDM measurements we were able to determine the lifetimes of two levels and limits on three others. We have already[6] discussed the measurement of the meanlife τ of the $(\nu f_{7/2})^3$, $\frac{15}{2}^-$ state at 2754 keV ($\tau = 34.1 \pm 1.5$ psec, see Table III) and will comment no further on it. The lower part of Fig. 3 illustrates the data we analyzed to obtain the lifetime of the 990-keV level. Our result is $\tau = 73 \pm 11$ psec, a value consistent with but a little higher than two previous measurements.[14,15] We take a weighted average of all three results to obtain the value of $\tau = 66 \pm 3$ psec given in Table III. We were able to obtain upper limits on the meanlives of the 2951-, 3371- and 3944-keV levels of 20, 20, and 5 psec, respectively, but were not able to extract a limit for the mean life of the 4591-keV level because the 647-keV line deexciting this state was very weak.

B. Results for ^{43}Sc

In an analysis similar to that used for ^{43}Ca we constructed the decay scheme for ^{43}Sc as shown in Fig. 2. Here again, the widths of arrows are proportional to the intensities of the transitions observed in the present work at a bombarding energy of 40 MeV. For the levels below 2.4 MeV and the 2553-keV level we take the spin-parity assignments of Endt and Van der Leun.[9] The levels at 2458, 3469, and 4361 keV, reported by Sawa[16] and indicated by dashed lines in Fig. 2 were not seen in the present work. The linear-polarization

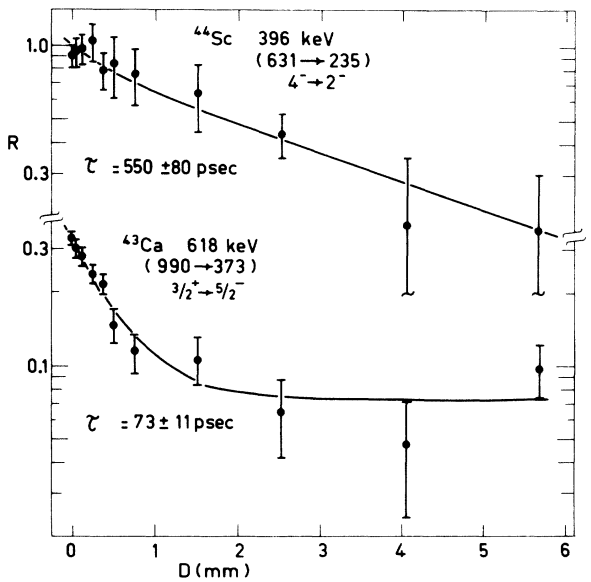

FIG. 3. The lower curve illustrates the RDM decay observed for the 617-keV transition from the 990- to the 373-keV level in ^{43}Ca, with $R = I_0/N$ as defined in the text. The abscissa is the target to stopper distance in mm. The upper curve illustrates the RDM decay observed for the $E2$ transition from the 631- to the 235-keV level in ^{44}Sc. Here $R = I_0/(I_0 + I_s)$.

results (see below) allow us to fix the parity of the level at 2987 keV, to which we assign $J^\pi = (\frac{15}{2})^-$. The spin-parity assignment to the 3123-keV level is from Ref. 17 and is based on γ-ray lifetime and angular distribution measurements. The spin-parity assignments to the states at 3141 and 3755 keV are based on the present work. The assignment for the 3141-keV level is in agreement with Kownacki *et al.*[16]; the 3755-keV level has not been previously observed. We summarize in Table II the data we have obtained on the γ-ray transitions in ^{43}Sc together with the results of other workers. (The format is the same as for Table I.) Most of the data in this table is in agreement with the spin-parity assignments of Fig. 2 except for two of the linear-polarization measurements. If the known mixing ratio ($x = 0.56 \pm 0.07$[18]) of the 729-keV transition from the 880-keV level is combined with the measured angular distribution, a linear polarization $P = 0.02 \pm 0.04$ is predicted, whereas the corresponding experimental quantity is $P_{exp} = 0.23 \pm 0.06$. A graph of P versus mixing ratio shows that the measured value of P_{exp} would correspond to a mixing ratio of $x \sim +1.5$. The sign of the mixing ratio which would be deduced from the polarization measurement is thus consistent with that deduced from the angular distribution analyses, but the magnitudes are in clear disagreement. The other problem concerns the linear polarization of the 1185-keV transition from the 1337-keV level. Although there is a large uncertainty in the value of P_{exp}, there is no overlap with the value of P predicted from the angular distribution. This is one of the weaker transitions observed, however, and could have a relatively large systematic error[2] due, for instance, to contamination by the strong ^{35}Cl γ ray[1] of 1184.80 ± 0.20 keV.

We were able to measure the lifetime of only one level in ^{43}Sc. The experimental results for the 880-keV level are presented in the lower part of Fig. 4: The mean life deduced from this data is $\tau = 7.0 \pm 1.4$ psec, in good agreement with two previous results[19,20] (see Table III). We take a weighted average of all three results to obtain a mean lifetime for this level of $\tau = 6.4 \pm 0.9$ psec. We were not able to obtain limits on the mean lives of the 3141- and 3755-keV levels: The γ rays deexciting these states were very weak in the RDM spectra.

The measured angular distributions and linear polarizations of the 1830- and 1158-keV γ rays determine odd parity for the 1830- and 2987-keV levels and are consistent with the spin-parity assignments of $(\frac{11}{2}^-)$ and $(\frac{15}{2}^-)$, respectively, set forth by Sawa, Sztarkier, and Bergstrom.[17] The results of Sawa *et al.*[17] then make an odd-parity assignment to the 3123-keV level highly probable.

The angular distribution and linear-polarization measurements on the 1209-keV γ ray from the 3141-keV level are consistent with it being a stretched $E2$ transition. We therefore make a tentative spin-parity assignment of $J^\pi = (\frac{13}{2})^+$ to the 3141-keV level. (Kownacki *et al.*[16] make a similar assignment.) The angular distribution and linear polarization of the 614-keV γ ray from the 3755-keV level are consistent with it being a

TABLE III. Lifetimes measured in the present work.

Nucleus	E_i (keV)	E_γ (keV)	Mean lifetime (psec) Present work	Other	Comments (Branching ratio)
^{40}Ca	4492	755	550 ± 110	392 ± 12 [a]	$E2$ $5^- \rightarrow 3^-$
^{43}Ca	2754	1076	34.1 ± 1.5	39 ± 5 [b]	$E2$ $(\frac{15}{2})^- \rightarrow \frac{11}{2}^-$
	990	618	73 ± 11	66 ± 4 [c] 65 ± 8 [d]	$E1$ $(\frac{3}{2})^+ \rightarrow \frac{5}{2}^-$ (88 ± 1%)
^{43}Sc	880	729	7.0 ± 1.4	$5.8^{+2.6}_{-1.5}$ [e] 6.0 ± 1.5 [f]	$M1/E2$ $\frac{5}{2}^+ \rightarrow \frac{3}{2}^+$
	472	472	233 ± 53	230 ± 20 [f,g]	$E2$ $\frac{3}{2}^- \rightarrow \frac{7}{2}^-$
^{44}Ca	3285	1002	23 ± 7	19.6 ± 1.7 [h]	$E2$ $6^+ \rightarrow 4^+$
	2283	1126	<25	<0.5 nsec [i]	$E2$ $4^+ \rightarrow 2^+$
^{44}Sc	631	396	550 ± 80	593 ± 43 [j]	$E2$ $(4)^- \rightarrow (2)^-$ (~45% [k,l])
	3567	896	51 ± 10	69.7 ± 2.4 [l]	$E2$ $(11)^+ \rightarrow (9)^+$

[a] Reference 17.
[b] K. P. Lieb and M. Uhrmacher, Z. Phys. 267, 399 (1974).
[c] Reference 14.
[d] Reference 15.
[e] Reference 19.
[f] Reference 20.
[g] References 9 and 20.
[h] Reference 22.
[i] Reference 23.
[j] Reference 24.
[k] Reference 1.
[l] Reference 5.

mixed $M1/E2$ transition $(\frac{15}{2})^+ \rightarrow (\frac{13}{2})^+$. We therefore suggest $J^\pi = (\frac{15}{2})^+$ for the level at 3755 keV.

C. Lifetimes in ^{40}Ca, ^{44}Ca, and ^{44}Sc

The nucleus ^{40}Ca was not excited very strongly with any of the target-projectile combinations studied. However, the 5^- state at 4492 keV was formed in the ^{19}F(^{27}Al, $\alpha 2n$)^{40}Ca reaction, albeit rather weakly. The mean life ($\tau = 550 \pm 110$ psec) obtained for this level is rather higher, and less accurate, than the result of a direct timing measurement by MacDonald *et al.*[21] which gave $\tau = 392 \pm 12$ psec.

The lowest 6^+ and 4^+ states in ^{44}Ca were populated quite weakly in the ^{27}Al(^{19}F,pn)^{44}Ca reaction. For the 6^+ state at 3285 keV our measured mean-life of 23 ± 7 psec is in good agreement with the result of Brown, Fossan, McDonald, and Snover[22] ($\tau = 19.6 \pm 1.7$ psec). Our results limit the mean-life of the 4^+ state at 2283 keV to $\tau < 25$ psec. A previous limit[23] was $\tau < 500$ psec.

The nucleus ^{44}Sc was formed strongly in the ^{28}Si(^{19}F, $2pn$)^{44}Sc reaction and results obtained are reported by Kolata, Olness, and Warburton.[5] It was much less abundantly produced in the ^{27}Al (^{19}F,pn)^{44}Sc reaction. We were, however, able to measure the mean life of the 631-keV level as $\tau = 550 \pm 80$ psec in good agreement with the result of Dracoulis, Durell, and Gelletly[24] of $\tau = 593 \pm 43$ psec. The data are shown in Fig. 3. Our result of $\tau = 51 \pm 10$ psec for the 3567-keV level is somewhat lower than the value of $\tau = 69.7 \pm 2.4$ psec reported in Ref. 5.

With respect to the lifetime measured for the 631-keV level, it should be remarked that the RDM measurements were undertaken at $E(^{19}\text{F}) = 36$ MeV, some 4 MeV less than the 40-MeV used in the angular distribution measurements. At this lower bombarding energy the 396-keV transition from the ^{44}Sc 631-keV state was observed to be much stronger than the 397-keV transition from ^{43}Ca. This was to be expected, since the two-particle emission channel should predominate at lower energies over the three-particle channel. The peak-fitting process was therefore able to reliably extract the intensity of the ^{44}Sc 396-keV line as a function of plunger distance: As seen in Fig. 3, there is no evidence for the 66 ± 3-psec lifetime associated with the ^{43}Ca 397-keV line.

IV. DISCUSSION

We first wish to discuss the high-spin states in ^{43}Ca and ^{43}Sc excited when ^{27}Al is bombarded by ^{19}F. As detailed above, the bracketed spin-parity assignments for the higher-lying levels in Figs. 1 and 2 must all be regarded as tentative as they are based on arguments which are dependent on the reaction mechanism. The point has, however, been covered before[7,11] and we will not belabor it. In most cases (specific exceptions have been discussed above) there are several pieces of experimental data all of which are in agreement with the bracketed spin-parity assignments. For ^{43}Ca we suggest on the basis of these arguments that the levels at 3944 and 4591 keV have $J^\pi = (\frac{15}{2}^+)$ and $(\frac{17}{2})$, respectively. The simple pairing force model discussed below predicts that the lowest $\frac{17}{2}^-$ state should be nearly 3 MeV higher in energy than the lowest $\frac{17}{2}^+$ state, which therefore supports the conclusion that the parity of the 4591-keV state is most probably even. If so, these states can be identified with the $\frac{17}{2}^+$ and $\frac{15}{2}^+$ states expected to arise from the $\nu(f_{7/2}{}^3, s=1)\pi(f_{7/2}d_{3/2}{}^{-1})$ configuration. Their energies suggest a further identification: They are the next two members of the even parity quasirotational band discussed by Alenius *et al.*[10] Whether the observed properties of this sequence of even-parity levels will be better explained by a rotational model or by a shell model is still a moot point, since other properties of these levels remain to be measured.[9] At present,

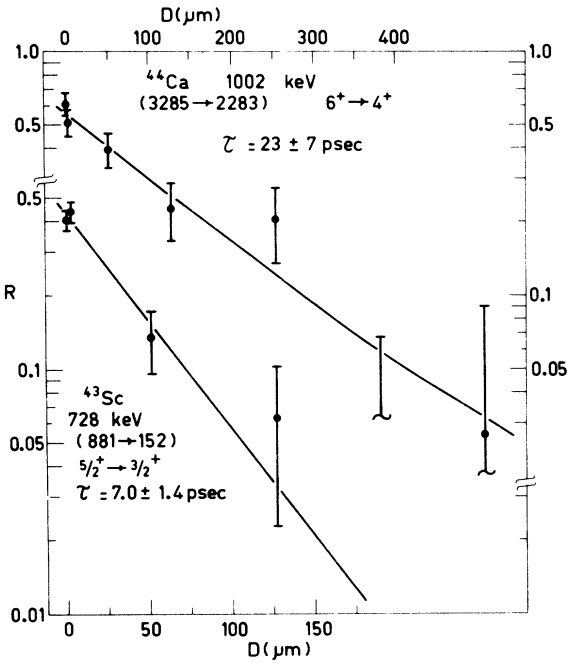

FIG. 4. The lower curve illustrates the RDM decay observed for the 728-keV transition from the 881-keV level in ^{43}Sc. The abscissa is the target to stopper distance in μm. The upper curve is for the RDM decay observed for the 1002-keV transition from the 3285-keV level in ^{44}Ca. For both cases $R = I_0/N$ as defined in the text.

of the seven possible mixed $M1/E2$ transitions connecting these levels, not one has been measured, while of the six possible $E2$ cross-over decays within the band only four are known. Finally, the mean lives of only the three lowest levels in the band have been determined. The odd-parity levels excited in the bombardment of ^{27}Al by ^{19}F can all be identified with levels belonging to the $\nu(f_{7/2}{}^3)$ configuration. We have already commented[6] on the application of the measurement of the lifetime of the 2754-keV level to the determination of effective charges in $E2$ transitions within $(f_{7/2}{}^n)$ configurations.

Shell model calculations[25] predict a spin sequence of $\frac{7}{2}^-$, $\frac{11}{2}^-$, $\frac{15}{2}^-$, and $\frac{19}{2}^-$ for the odd-parity states in ^{43}Sc arising primarily from the $\nu(f_{7/2}{}^2)\pi(f_{7/2})$ configuration. As mentioned above, we have been able to fix the parity of the level at 2987 keV as odd, while the level at 3123 keV almost certainly has the same parity. These two levels, strongly fed in the fusion-evaporation reaction, are therefore to be identified, with a very high probability, with the two high-spin levels arising mainly from the $f_{7/2}{}^3$ configuration. As was the case also for ^{43}Ca, a series of even-parity states in ^{43}Sc is also populated, comprising a quasi-rotational band based on the $\frac{3}{2}^+$ level at 152 keV. The properties of the states in this band are better established than is the case for ^{43}Ca. Our results allow us to fix the parity of the levels at 3141 and 3755 keV as even which, in conjunction with the probable spin assignments of $(\frac{13}{2})$ and $(\frac{15}{2})$, respectively, extends the sequence of levels in the even-parity band to $J^\pi = \frac{15}{2}^+$. For the lower-lying members of this band, Maurenzig[26] compares the results of Johnstone's calculations[27] with experiment. To further test the model, lifetime measurements of the higher excited states and a determination of the mixing and branching ratios of the transitions deexciting them are needed.

There is an abundance of data concerning the ^{19}F + ^{27}Al fusion-evaporation reaction contained in the relative γ-ray excitation intensities listed in Ref. 1 and Tables I to III. In this section we wish to gather these data together in such a way as to be able to draw from it some relevant generalizations and compare it with statistical-model calculations of cross sections for forming the residual nuclei. As a first step we list in Table IV the γ rays which signal the excitation of a given product nucleus and whose intensities, when summed, give the total excitation of that nucleus via the ^{19}F + ^{27}Al fusion-evaporation reaction. As an example to illustrate the method of construction, consider the entry for ^{43}Ca. From the excitation and decay diagram (Fig. 1), the γ rays signaling excitation of this nucleus are those of 1678, 2094, 373, 593, 1902, and 2410 keV. However, the 373-keV transition is fed strongly in the β decay of ^{43}Sc, so that it is replaced by the sum of the intensities of the γ-ray lines of 221, 1022, and 618 keV. Excitation of ^{43}K was not observed, and

TABLE IV. Relative excitation of residual nuclei in the bombardment of ^{27}Al by ^{19}F at 40 MeV.

Nucleus	Characteristic γ rays, E_γ (keV)	Intensity
^{45}Ti + n		...
^{44}Ti + 2n	1083	1700
^{43}Ti + 3n		...
^{45}Sc + p	1237 + 543 + 531 + 975 + 962	...
^{44}Sc + pn	235 + 350 + 357 + 425 + 531 + 697 + 926	14 800
^{43}Sc + $p2n$	729 + 1185 + 472 + 1830 + (2458)	63 500
^{44}Ca + 2p	1156 (or 1126)	<18 480, >3850 [a]
^{43}Ca + 2pn	1678 + 2094 + 593 + 220 + 1022 + 617 + 1902 + 2410	<81 460, >50 680 [b]
^{42}Ca + 2$p2n$	1524	14 590
^{41}Ca + αn	3201 + 3369	12 000
^{40}Ca + $\alpha 2n$	3737 + 3904	6770
^{42}K + 3pn	107 (or 151)	$\lesssim$3630
^{41}K + αp	1293 + 1677 (or 851)	<40 900, >15 200 [c]
^{40}K + αpn	891 (or 1651)	<44 100, >36 400 [d]
^{40}Ar + $\alpha 2p$	1460	2250
^{38}Ar + 2α	2167 (or 1642)	9350
^{37}Ar + 2αn	1611 (or 1573 + 2095 (or 0.86 × 1506)) + 2217	1400
^{37}Cl + 2αp	3087 + 3103 + 4010	1400

[a] Direct excitation (excluding feeding by β decay) is close to this lower limit.
[b] Estimated to be 68 000 for the purposes of illustration in Fig. 5.
[c] Estimated to be 15 200 for the purposes of illustration in Fig. 5.
[d] Estimated to be 40 000 for the purposes of illustration in Fig. 5.

Hence no allowance was made for its decay to excited states of ^{43}Ca. Similar considerations were made in compiling the list for the other nuclei in the table.

With this list, the intensities of excitation of individual γ-ray transitions could then be converted to intensities of excitation of the individual nuclei. The results of this computation are given in the last column of Table IV. We neglect direct excitation of the ground states, so that our results therefore strictly apply only to excitation via the yrast levels. However, general consideration of the fusion-evaporation reaction mechanism suggests that such direct excitation of the ground state should in most cases be very small. For some of the entries in Table IV we could only put limits on the excitation because of interference from γ rays of the same or similar energy in other nuclei. The relative excitation intensities are displayed in graphical form in Fig. 5. In this figure, the X and Y coordinates are, respectively, the atomic number and excitation energy of the residual nucleus, while the Z coordinate gives the intensity of excitation in arbitrary units. The height of the right-hand side of each block represents the experimentally observed relative excitation as derived from Table IV. The height of the left-hand side of each block represents the cross section for excitation as determined in a statistical-model calculation which we discuss below. The nuclei excited by the ^{19}F + ^{27}Al reaction fall naturally, in the diagram, into three groups: The one in the middle which contains the three most strongly excited nuclei corresponds to three-particle emission. The group at the lower left-hand corner corresponds to two particle emission. The members of this group are on the average more weakly excited than the nuclei corresponding to three-particle emission. ^{42}Ca and ^{42}K in the upper right-hand corner correspond to four-particle emission and are quite weakly excited.

We now wish to compare the experimental cross sections for excitation of the nuclei listed in Table IV and displayed in Fig. 5 with a statistical-model calculation. For this purpose the nuclear evaporation code[28] GROGI2 was used. This code, based on an earlier spin dependent nuclear evaporation program,[29] follows the deexcitation of the compound nucleus via neutron, proton, α, and photon emission channels. Hence the cross section for excitation of any particular nucleus can be obtained. Input parameters for the calculation were taken as follows: transmission coefficients for the neutron, proton, and α particles and the heavy ions were determined from average optical-model parameters taken from the literature. Q values for particle evaporation at each step were taken from the compilation of Wapstra and Gove,[30] while

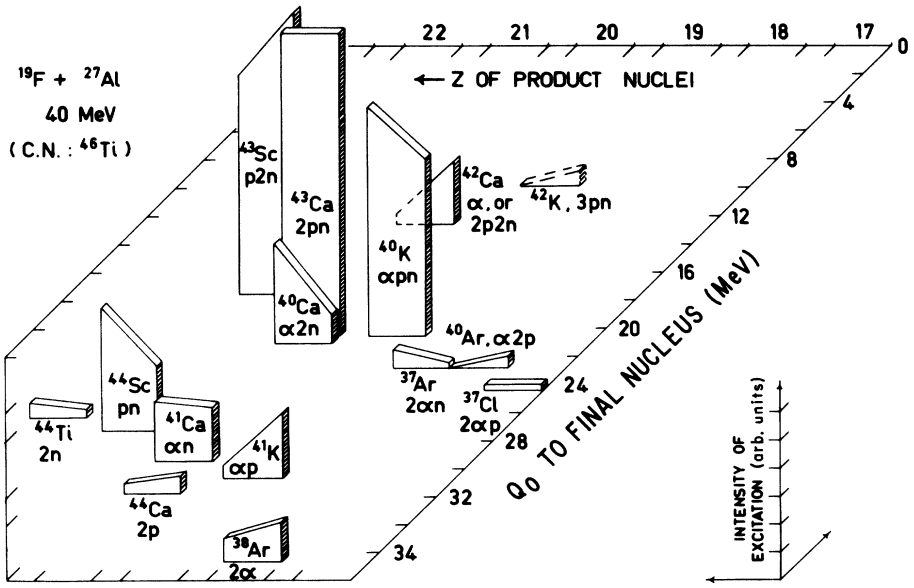

FIG. 5. Comparison of the excitation intensities observed for the residual nuclei populated by the bombardment of ^{27}Al by 40-MeV ^{19}F ions with statistical model calculations of cross sections for formation of the same nuclei (see text for details). The X and Y coordinates are, respectively, the atomic number and excitation energy of the residual nucleus, while the Z coordinate gives the intensity of excitation in arbitrary units. Height of right-hand side of each block represents observed excitation intensity, while the left-hand side represents the calculated cross section for formation of the same nucleus. Relative excitation intensities are also listed in Tables IV and V.

the level density parameters we used are due to Facchini and Saetta-Menichella.[31] The energies of the yrast levels were calculated using a rotational model with a rigid body moment of inertia for a sphere of radius $1.2A^{1/3}$ fm. Only dipole or quadrupole photon deexcitations are considered by the code. We took the dipole-width parameter to be 1.2×10^{-7} and the quadrupole-width parameter to be 3.5×10^{-10} [32,33] These values correspond to a dipole width of 1 eV for a transition from a state in the compound nucleus at the neutron binding energy, and to a ratio of dipole/quadrupole strengths of 5×10^{-3}.

The cross sections (in mb) for forming the various possible residual nuclei following the bombardment of ^{27}Al with ^{19}F at 40 MeV as calculated using GROGI2 are given in the second column of Table V. In order to compare these predicted cross-sections with the relative intensities given in Table IV we normalize the total intensity from Table IV to the total calculated cross section in Table V and present these relative cross sections in the last column of that table. In addition, in Fig. 5 we display the calculated cross sections as the height of the left-hand side of each block in order to compare them for each nucleus with the relative experimental intensities. A glance at Fig. 5 immediately indicates the success of the statistical model calculation. The strong population of ^{43}Sc, ^{43}Ca, and ^{40}K is well reproduced as is the relatively weaker population of the other nuclei obtained by three particle emission, with the possible exception of ^{40}Ca. The intermediate intensity of population of the nuclei obtained by two-particle emission is also well reproduced again with one possible exception—^{41}K.

TABLE V. Comparison of excitation cross sections as calculated using statistical (Hauser-Feshbach) theory and relative observed cross sections. The calculated cross sections are in mb, whereas the experimental cross sections are only relative. Reaction: ^{19}F + ^{27}Al at 40 MeV.

Residual nucleus	H-F (mb)	Experimental
^{44}Ti + $2n$	8.7	4.3
^{44}Sc + pn	69.2	36.3
^{43}Sc + $p2n$	121.0	155.6
^{44}Ca + $2p$	6.2	9.4
^{43}Ca + $2pn$	169	166.77
^{42}Ca + $2p2n$ or α	6.4	35.8
^{41}Ca + αn	33.7	29.4
^{40}Ca + $\alpha 2n$	56.4	16.4
^{42}K + $3pn$	0	8.8
^{41}K + αp	8.0	37.3
^{40}K + αpn	126.6	98.0
^{40}Ar + $\alpha 2p$	0.2	5.4
^{38}Ar + 2α	13.5	22.9
^{37}Ar + $2\alpha n$	10.9	3.3
^{37}Cl + $2\alpha p$	3.2	3.3

The statistical model makes no distinction between levels of odd or even parity. It is a matter of observation, however, that intensities of excitation differ radically between the yrast levels of opposite parity. In order to further understand some of these features we invoke a very simple model to calculate the excitation energies of the yrast levels in the residual nuclei. The model is a pairing force one; however, we simplify it by assuming that an interparticle interaction occurs only when the particles are in the same orbit. For this we take the energies calculated from the pairing force interaction as[34]

$$E_{N,s} = -\,|G|\,(N-s)(2\Omega - N - s + 2)/4\,, \qquad (1)$$

where N is the number of particles in the given orbit, s is the seniority, and Ω is the number of pair states available in the orbit. $|G|$ is the strength of the pairing force interaction. We further simplify the treatment by assuming there is no interaction between protons and neutrons.

We assume that $|G|$ can vary, depending on the orbit. Furthermore, we will use empirical data to determine $|G|$. In this region of the Periodic Table, the lowest-lying levels for spins in the region of $J = 8$ to 16 are obtained by maximizing the number of particles in the $f_{7/2}$ shell. Consequently, it is only the value of $|G|$ for the $d_{3/2}$ and $f_{7/2}$ orbits which we need to determine. For the $d_{3/2}$ shell we can use the energies of the first excited states of ^{34}S or ^{38}Ar. In both cases

$$E_{2,2} - E_{2,0} = 2\,|G|\,.$$

The excited state energies are, respectively, 2.13 and 2.17 MeV; we therefore take $|G|$ for the $d_{3/2}$ orbit as $G_{3/2} = 1.08$ MeV. For the $f_{7/2}$ shell an estimate of $|G|$ can be obtained by taking a spin weighted average of the energies of all states of a given seniority as defining $E_{N,s}$ and thus $G_{7/2}$. For the purpose of our calculation we took $G_{7/2} = 0.62$ MeV. Finally, the difference in energy, $\epsilon = \epsilon_{7/2} - \epsilon_{3/2}$, between the $f_{7/2}$ and $d_{3/2}$ single particle orbits was determined from the excitation energy of the lowest $\frac{7}{2}^-$ level in ^{39}K and ^{39}Ca. Within our model this energy difference is given by

$$E_{7/2} - E_{3/2} = \epsilon + (E_{1,1})_{7/2} + (E_{2,0})_{3/2} - (E_{3,1})_{3/2}$$
$$= \epsilon - G_{3/2}\,.$$

Since $E_{7/2} - E_{3/2} = 2.80$ MeV and $G_{3/2} = 1.08$ MeV, $\epsilon = 3.88$ MeV. We can now write the energy of a state of a given configuration as

$$E = \sum_{j_p} \left[(E_{N,s})_{j_p} + \epsilon_{j_p}\right] + \sum_{j_n} \left[(E_{N,s})_{j_n} + \epsilon_{j_n}\right]. \qquad (2)$$

The possible spins are determined according to the usual coupling rules. The yrast levels arise from the configurations which give the lowest energy for a given total angular momentum.

Tables VI–VIII give the results obtained by using Eqs. (1) and (2) to calculate the energies of the odd-and even-parity yrast levels in the nuclei of interest. We will now use the data summarized in Tables VI–VIII to interpret a number of empirical observations in specific nuclei.

A. Nuclei ^{43}Ca and ^{43}Sc

A comparison with Figs. 1 and 2 allows us to understand a number of features seen in these diagrams. That no odd-parity level with $J>\frac{15}{2}$ is observed in ^{43}Ca is explained by the large energy gap predicted by the model above this spin. The even-parity levels, however, appear to be populated up to $J=\frac{17}{2}$. That no even-parity level with higher spin has been seen correlates well with the energy gap predicted above this level. The model predicts that the rather regular energy spacing between these even-parity levels will not persist past $J=\frac{17}{2}$. The model predicts the lack of any observed transitions from the $(\frac{17}{2}^+)$ or $(\frac{15}{2}^+)$ levels to the $\frac{15}{2}^-$ level, since the even-parity states arise from the $\pi(f_{7/2}d_{3/2}{}^{-1})\nu(f_{7/2}{}^3, s=1)$ configuration, while the $(\frac{15}{2})^-$ level arises from the $\nu(f_{7/2}{}^3, s=3)$ configuration. The rather weak $E1$ transition from the $(\frac{13}{2}^+)$ state to the $(\frac{15}{2})^-$ level can only be understood in terms of further admixtures to these simple states. In the case of ^{43}Sc we of course expect to observe the $(\frac{19}{2})^-$ state, since this arises from the low-lying $\pi(f_{7/2})\nu(f_{7/2}{}^2)$ configuration. In addition, although we have observed only up to $(\frac{15}{2})^+$, at a somewhat higher bombarding energy we would expect to observe the $\frac{17}{2}^+$ level at approximately 4360 keV excitation but would not expect to see a $\frac{19}{2}^+$ level except at a considerably higher energy because of the gap between these two spins which occurs in the simple model.

B. Nuclei ^{41}K and ^{41}Ca

For ^{41}K the nonobservation[3] of high-spin levels above the $(\frac{19}{2}^-)$ and $(\frac{15}{2}^+)$ levels is explained by the energy gaps above both levels in the model. (Apparently the $J^\pi=\frac{5}{2}^-$, $\frac{9}{2}^-$, $\frac{13}{2}^-$, and $\frac{17}{2}^-$ levels lie, respectively, above the $J^\pi=\frac{7}{2}^-$, $\frac{11}{2}^-$, $\frac{15}{2}^-$, and $\frac{19}{2}^-$ levels and are therefore not excited.) The $E1$ transition from the $(\frac{15}{2}^-)$ to the $(\frac{13}{2}^+)$ level is forbidden by the simple model. [Their configurations are, respectively, $\nu(f_{7/2}{}^2, s=2)\pi(f_{7/2}d_{3/2}{}^{-2})$ and $\nu(f_{7/2}{}^2, s=2)\pi(d_{3/2}{}^{-1})$ which explains why the $E2$ transition to the $(\frac{11}{2}^-)$ level can compete successfully with the $E1$ transition to the $(\frac{13}{2}^+)$ level.] In ^{41}Ca the $E1$ transition from the $\frac{19}{2}^-$ to the $\frac{17}{2}^+$ level is forbidden [experimentally[3] $|E1|^2<10^{-3}$ W.u. (Weisskopf units)]. In addition, since the model predicts that the odd-parity levels with $J=\frac{21}{2}$ to $\frac{25}{2}$ lie lower than the corresponding even-parity levels, the $\frac{19}{2}^-$ level should collect all of the strength of the cascade down the yrast line. This

TABLE VI. Yrast level energies in MeV calculated using the simple pairing force model. The asterisk designates the highest-spin state observed or suggested from experimental data.

Nucleus	^{41}K		^{41}Ca		^{43}Ca		^{43}Sc	
$2J$/	E_J^+	E_J^-	E_J^+	E_J^-	E_J^+	E_J^-	E_J^+	E_J^-
1/	2.5	5.6	5.0	7.4	5.0	7.4	5.0	
3/	0.0	5.0	2.5	7.4	3.1	1.9	2.5	2.5
5/	2.5	5.0	5.0	7.4	5.0	1.9	5.0	2.5
7/	2.5	2.8	5.0	0.0	5.0	0.0	5.0	0.0
9/	2.5	5.0	5.0	7.4	5.0	1.9	5.0	2.5
11/	2.5	5.0	5.0	7.4	5.0	1.9	5.0	2.5
13/	2.5	5.3	5.0	7.4	5.0	8.1	5.0	2.5
15/	2.5*	5.3	5.0	7.8	5.0	1.9*	5.0	2.5
17/	8.4	5.3	5.0*	7.8	5.0*	7.8	5.6*	2.5
19/	10.2	5.3*	12.4	7.8*	6.8	7.8	7.4	2.5*
21/	10.2	7.4	12.7	9.9	6.8	9.6	7.4	9.9
23/	10.2	7.4	12.7	9.9	6.8	9.6	7.4	10.2
25/	10.2	14.4	12.7	9.9	6.8	9.6	7.4	10.2
27/	10.2	15.2	12.7	15.5	13.3	9.6	7.4	10.2
29/	12.4	16.3	14.9	17.7	14.6	11.8	15.2	12.4
31/	19.1	16.3	14.9	17.7	14.6	19.4	15.2	12.4
33/	20.2	16.3	21.6	18.8	14.6	19.4	15.2	12.4
35/	21.2	25.1	23.7	19.8	16.8	20.6	16.3	20.2
37/			23.7	27.6	25.0	20.6	17.4	21.2
39/							26.2	22.3

TABLE VII. Yrast level energies in MeV calculated using the simple pairing force model. The asterisk designates the highest-spin state observed or suggested from experimental data.

Nucleus	^{40}Ar		^{40}K		^{40}Ca	
J	E_J^+	E_J^-	E_J^+	E_J^-	E_J^+	E_J^-
0	0.0		5.0		0.0	12.7
1	4.6		2.5		9.9	12.7
2	2.2	5.6	5.0	0.0	7.8	5.0
3	4.6	5.6	2.5	0.0	9.9	5.0
4	2.5	5.6	5.0	0.0	7.8	5.0
5	4.6	5.6*	2.8	0.0*	9.9	5.0*
6	2.5*	7.4	5.0	7.4	7.8	12.7
7	4.6	7.4	2.8*	7.4	9.9	12.7
8	4.6	7.4	5.0	7.8	9.9*	12.7
9	11.6	7.4	5.0	7.8	9.9	12.7
10	11.6	8.5	10.6	7.8	9.9	12.7
11	12.4	8.5	10.6	7.8	12.7	12.7
12	12.4	16.3	12.7	9.9	13.9	14.9
13	13.5	16.3	12.7	9.9	13.9	14.9
14	13.5	17.4	13.8	16.6	17.7	21.6
15	22.3	17.4	13.8	16.6	19.8	21.6
16	22.3		22.6	18.8	19.8	23.7
17			22.6	18.8	27.6	23.7
18					27.6	

TABLE VIII. Yrast level energies in MeV calculated using the simple pairing force model. The asterisk designates the highest-spin state observed or suggested from experimental data.

Nucleus	^{38}Ar		^{42}Ca	
J	E_J^+	E_J^-	E_J^+	E_J^-
0	0.0	7.1	0.0	7.4
1	9.6	7.1	12.4	7.4
2	2.2	5.0	2.5	5.0
3	9.6	5.0	12.4	5.0
4	7.8	5.0	2.5	5.0
5	9.9	5.0	10.2	5.0
6	7.8	7.1	2.5*	7.4
7	9.9	7.1	12.4	7.4
8	9.9*	13.8	10.2	7.4
9	11.0	13.8	10.5	7.4
10	11.0	13.8	10.5	7.4
11	19.8	13.8*	12.4	7.4*
12	19.8	16.0	12.4	15.2
13	19.8	16.0	12.4	15.2
14	19.8	23.7	12.4	15.2
15		23.7	20.2	15.2
16			20.2	17.4
17			21.2	17.4
18			21.2	26.2
19				26.2

is indeed observed. Again the model predicts that for $J=\frac{9}{2}$ to $\frac{17}{2}$ the even-parity levels will lie lower than the corresponding odd-parity levels. This explains why the five even-parity levels are populated in the cascade from the $(\frac{19}{2}^-)$ level.

C. Nuclei ^{40}Ar, ^{40}K, and ^{40}Ca

For ^{40}Ar we infer the excitation of the 6^+ state at 3.46 MeV and expect it to be fed from either the $J^\pi = 7^+$ or 8^+ state at an excitation of roughly 2 MeV higher. We would expect these two upper states to be fed in turn by a cascade from the $J^\pi = 8^-$ or 9^- states predicted to lie in the vicinity of 7.4 MeV. The very weak formation of high-spin states in ^{40}Ca above the well known 5^- state at 4.49 MeV is explained by the large energy gap above this level. Recently γ rays with energies of 1168.86 ± 0.35 and 1374.30 ± 0.20 keV observed in ^{19}F + ^{24}Mg and ^{16}O + ^{27}Al fusion-evaporation reactions[1] have been identified[35,36] via ^{14}N + ^{28}Si $\gamma\gamma$-coincidence experiments as arising from a cascade in ^{40}Ca: $8098 \xrightarrow{1169} 6929 \xrightarrow{1651} 5278 \xrightarrow{1374} 3904$ keV with the second γ ray of 1651 keV degenerate with a much stronger one from ^{40}K. The 8098- and 6929-keV levels are strong candidates for 8^+ and 6^+ states.[35,36] The γ rays deexciting them were not observed in the ^{27}Al(^{19}F, $\alpha 2n$)^{40}Ca reaction. For ^{40}K the excitation of the 5^- state through the 7^+ state is explained by their relative energies and the high excitation energies of the 6^- to 9^- states. We would expect the 6^+ and 7^+ states to be fed from the 8^+ and 9^+ levels which should lie within an MeV or so of the 6^+ level.

D. Nucleus ^{38}Ar

The 9^+ and 10^+ and 8^- to 11^- states of the simple model are all reasonable condidates for the high-spin states seen[8] in ^{38}Ar. In addition a comparison of the experimental spectrum of, say, ^{44}Ti with that of ^{38}Ar illustrates that a much higher energy is needed to reach, say, $J = 10$ in ^{38}Ar than in ^{44}Ti. The model is in agreement with this observation.

The hospitality extended to A. R. Poletti by the Physics Department at Brookhaven National Laboratory is warmly appreciated.

†Research supported by the U. S. Energy Research and Development Administration and the N.Z. University Research Grants Committee.

*Visiting physicist, Brookhaven National Laboratory, January–May 1973.

‡Present address: Laboratoire Spectrometrie Nucléaire, Strasbourg, France.

[1]E. K. Warburton, J. J. Kolata, J. W. Olness, A. R. Poletti, and Ph. Gorodetzky, At. Data Nucl. Data Tables 14, 147 (1974).

[2]J. W. Olness, A. H. Lumpkin, J. J. Kolata, E. K. Warburton, J. S. Kim, and Y. K. Lee, Phys. Rev. C 11, 110 (1975).

[3]P. Gorodetzky, J. J. Kolata, J. W. Olness, A. R. Poletti, and E. K. Warburton, Phys. Rev. Lett. 31, 1067 (1973).

[4]J. J. Kolata, Ph. Gorodetzky, J. W. Olness, A. R. Poletti, and E. K. Warburton, Phys. Rev. C 9, 953 (1974).

[5]J. J. Kolata, J. W. Olness, and E. K. Warburton, Phys. Rev. C 10, 1663 (1974).

[6]A. R. Poletti, B. A. Brown, D. B. Fossan, P. Gorodetzky, J. J. Kolata, J. W. Olness, and E. K. Warburton, Phys. Rev. C 10, 997 (1974).

[7]E. K. Warburton, J. J. Kolata, and J. W. Olness, Phys. Rev. C 11, 700 (1975).

[8]E. K. Warburton, J. J. Kolata, and J. W. Olness, Bull. Am. Phys. Soc. 20, 732 (1975); J. J. Kolata, J. W. Olness, E. K. Warburton, and A. R. Poletti, Phys. Rev. C (to be published).

[9]P. M. Endt and C. Van der Leun, Nucl. Phys. A214, 1 (1973).

[10]N. G. Alenius, S. E. Arnell, Ö. Skeppstedt, E. Wallander, and Z. P. Sawa, Nuovo Cimento 8A, 147 (1972).

[11]A. R. Poletti, B. A. Brown, D. B. Fossan, and E. K. Warburton, Phys. Rev. C 10, 2312 (1974).

[12]P. Taras and B. Haas, Nucl. Instrum. Methods 123, 73 (1975).

[13]H. Gruppelaar and P. J. M. Smulders, Nucl. Phys. A179, 737(1972).

[14]M. Bini, P. G Bizzeti, A. M. Bizzeti-Sona, and R. A. Ricci, Phys. Rev. C 6, 784 (1972).

[15]R. W. Kavanagh, N. Schultz, and J. C. Merdinger, Nucl. Phys. A195, 302 (1972).

[16]Z. P. Sawa, A. F. I. 1972 Annual Report No. 3. 2. 7 (unpublished); J. Kownacki, L. Harms-Ringdahl, J. Sztarkier, and Z. P. Sawa, A. F. I. 1972 Annual Report No. 3. 2. 9 (unpublished).

[17]Z. Sawa, J. Sztarkier and I. Bergström, Phys. Scr. 2, 261 (1970); K. Nakai, B. Skaali, N. J. Sigurd Hansen, B. Herskind, and Z. Sawa, Phys. Rev. Lett. 27, 155 (1971).

[18]A weighted average of results quoted by G. C. Ball, J. S. Forster, F. Ingebretsen, and C. F. Monahan, Can. J. Phys. 48, 2735 (1970); J. C. Manthuruthil, C. P. Poirier and J. Walinga, Phys. Rev. C 1, 507 (1970).

[19]G. C. Ball, J. S. Forster, F. Ingebretsen, and C. F. Monahan, Nucl. Phys. A180, 517 (1972).

[20]G. C. Ball, J. S. Forster, D. Ward, and C. F. Monahan, Phys. Lett. 37B, 366 (1971).

[21]J. R. MacDonald, N. Benczer-Koller, J. Tape, L. Guthman, and P. Goode, Phys. Rev. Lett. 23, 594 (1969).

[22]B. A. Brown, D. B. Fossan, J. M. McDonald, and K. A. Snover, Phys. Rev. C 9, 1033 (1974).

[23]D. H. White and R. E. Birkett, Phys. Rev. C 5, 513 (1972).

[24]G. D. Dracoulis, J. L. Durell, and W. Gelletly, J. Phys. A 6, 1030 (1973).

[25]L. Zamick, in *The Structure of $1f_{7/2}$ Nuclei*, edited by R. A. Ricci (Editrice, Bologna, 1971), p. 9 and cited references.

[26]P. R. Maurenzig, in *The Structure of $1f_{7/2}$ Nuclei* (see Ref. 25), p. 469.

[27]As reported by J. S. Forster, G. C. Ball, F. Ingebretsen, and C. F. Monahan, Phys. Lett. 32B, 451 (1970).

[28]GROGI2—A Nuclear Evaporation Computer Code, J. Gilat, BNL Report No. 50246, 1970 (unpublished).

[29]J. R. Grover and J. Gilat, Phys. Rev. 157, 802 (1967).

[30]A. H. Wapstra and N. B. Gove, Nucl. Data A9, 267 (1971).

[31]U. Facchini and E. Saetta-Menichella, Energ. Nucl. (Milan) 15, 54 (1968).

[32]J. J. Kolata, J. W. Olness, and E. K. Warburton (unpublished).

[33]See for discussion: J. Dauk, K. P. Lieb, and A. M. Kleinfeld, Nucl. Phys. A241, 170 (1975).

[34]A. M. Lane, *Nuclear Theory* (Benjamin, New York, 1964).

[35]J. J. Simpson, S. J. Wilson, P. W. Green, J. A. Kuehner, W. R. Dixon, and R. S. Storey, Phys. Rev. Lett. 35, 23 (1975).

[36]J. J. Kolata and A. M. Nathan (private communication).

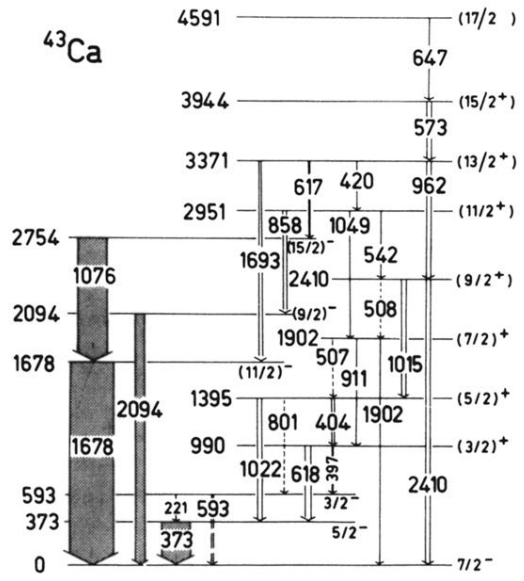

FIG. 1. The level scheme of ^{43}Ca as deduced from its excitation by the ^{27}Al(^{19}F, $n2p$)^{43}Ca reaction at 40 MeV. The widths of the arrows signifying observed transitions are proportional to their relative intensities. Transitions reported by other workers and indicated by dashed lines were too weak to be observed in the present experiments.

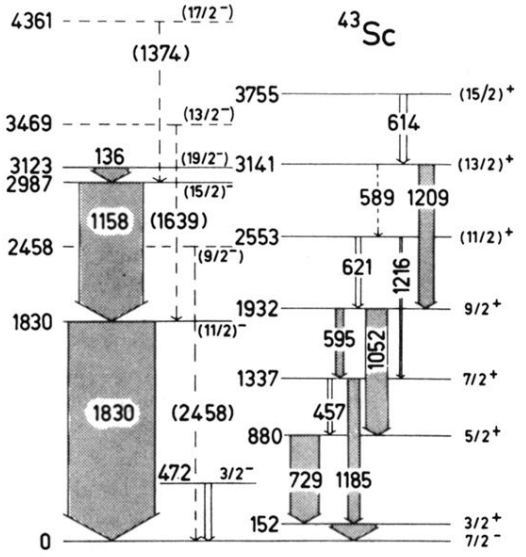

FIG. 2. The level scheme of ^{43}Sc as deduced from its excitation by the ^{27}Al(^{19}F, $2np$)^{43}Sc reaction at 40 MeV. The widths of the arrows signifying observed transitions are proportional to their relative intensities. Three high-spin states and their γ-ray decays reported by other workers, but too weak to be observed in the present experiment, are indicated by dashed lines.